ORIGINAL RESEARCH

Antibacterial effects of silver–zirconia composite coatings using pulsed laser deposition onto 316L SS for bio implants

G. Pradhaban · Gobi Saravanan Kaliaraj · Vinita Vishwakarma

Abstract Bacterial invasion on biomedical implants is a challenging task for long-term and permanent implant fixations. Prevention of initial bacterial adherence on metallic implants is an important concern to avoid extracellular matrix (biofilm) secretion from bacteria that is resistant to antibacterial agents. In order to overcome this defect, recently, surface coatings such as zirconia (ZrO_2) with higher smoothness have been shown to improve implants durability. In the present study, pulsed laser deposition (PLD) was used to deposit ZrO_2 and silver (Ag)-ZrO_2 composite coatings onto 316L stainless steel (316L SS). Phase purity, surface roughness and surface morphology, thickness of the coatings and elemental compositions of the coatings were analyzed using X-ray diffraction (XRD), atomic force microscopy (AFM) and scanning electron microscopy (SEM) with energy dispersive X-ray spectroscopy (EDS). Total viable count (TVC) and epifluorescence microscopy analysis were studied to evaluate antimicrobial efficiency of ZrO_2 and Ag–ZrO_2 composite coatings using gram negative (gram −ve) *Escherichia coli* (*E.coli*) and gram positive (gram +ve) *Staphylococcus aureus* (*S.aureus*). On the basis of the present study, it could be speculated that ZrO_2 coatings exhibited antibacterial activity against only *E.coli*, whereas Ag–ZrO_2 composite coatings showed superior activity against *E.coli* and *S.aureus* strains.

Keywords Zirconia · Silver · Biomedical implants · Thin films · PLD · Antibacterial effect

G. Pradhaban · G. S. Kaliaraj (✉) · V. Vishwakarma
Centre for Nanoscience and Nanotechnology, Sathyabama University, Chennai 600119, India
e-mail: gsnanotech@gmail.com

Introduction

In recent years, the number of implant devices have increased for various implant surgeries takes leading effort across the world (Nathan et al. 2012). The demands of implants have significantly increased not only for new patients but also for patients who must receive revision surgeries. After implantation, the implant materials should not cause allergic and hypersensitive reactions. Hence, biocompatibility is an essential requirement for an artificial implant to exhibit chemical bonding to living tissues upon the formation of bone-like apatite layer on its surface in any simulated body environment (Kokubo 2008; Arisara et al. 2012). In order to improve bioactivity, biocompatibility and implant longevity, thin films which are having nano crystalline achieved considerable breakthrough in the field of biomedical sciences due to their exceptional physical and chemical properties (Holleck 1991). Nanostructured metal oxide thin films and metal complexes have emerged as class materials which are increasingly being studied for health-related applications. Highly ionic metal oxides are interesting in physical, chemical and antibacterial properties (Gu et al. 2007; Jangra et al. 2012).

Among various metal oxides, ZrO_2 is used extensively for various implant devices because of its good mechanical and biocompatibility properties and used for esthetic devices too. As a ceramic, ZrO_2 exhibits several advantages such as corrosion resistance, mechanical strength and fracture toughness. The enhanced properties of ZrO_2 attributed to high crystallinity and nano crystalline ZrO_2 express better biocompatibility and bioactivity nature (Uchida et al. 2002). The requirement of ZrO_2 implants have been increased significantly from 4, 28,000 to 2.16

Springer

million per year for total knee arthroplasty. Hip replacement is also one of the important applications of ZrO_2 among the various implants. Chevalior stated that more than 6,00,000 ZrO_2 femoral have been implanted worldwide (Chevalier 2006). The ceramic ZrO_2 implant materials, with ISO standard No. 13356, are extensively being used. Even though ZrO_2 thin films are near ideal biomaterial, their use does not always guarantee adequate results. In this aspect, Microbial invasion and colonization on ZrO_2 implant materials is still a major challenge against implant durability. Since ZrO_2 thin film exhibits antibacterial activity against only *E.coli*, it is not active against a wide variety of microbial species and thereby implanted material is prone to bacterial attack that may eventually lead to inflammation and destructive of the implants (Jangra et al. 2012). Among the various bacterial species *Enterococcus faecalis*, *E.Coli*, *Cornybacterium* sp., and *Staphylococcus* sp., predominantly invade the implant materials and cause orthopedic infections (Udo 2009). Hence, microbial invasion is an important crisis for implant success and durability. Diagnosis and treatment for implant failure is the tedious process in case of load bearing and hip, knee artroplasty implants. Recently, addition of antimicrobial metallic materials into metal oxide implants is suitable choice to elevate the antimicrobial property, especially from implant-associated infectious bacteria (Jelinek et al. 2013). In that perspective, Silver has been used in many medical devices such as bone cements, catheters, orthopedic fixation pins, dental implants, and cardiac prostheses (Lansdown 2006). One of the best known uses of silver in medicine is to serve as the primary antimicrobial agent in topical creams to heal severe burns (Lansdown 2007; Atiyeh et al. 2007). Since bacterial infections are associated with prosthetic failures, silver has been considered as a medical coating for broad range of microbial inactivation. Since hydroxyapatite has poor mechanical property, Ag–ZrO_2 thin composite coatings are studied extensively to enhance biocompatibility, mechanical, and antimicrobial behavior. Ag–ZrO_2 thin composite coatings have been fabricated using several methods such as sol–gel, physical vapor deposition, and plasma spraying (Ewald et al. 2006; Zheng et al. 2009; Chen et al. 2007). Among the various deposition techniques, pulsed laser deposition (PLD) is one of the novel methods to modify the metal surface. It gives high deposition rate, good stoichiometry, and better adhesion. In this work, ZrO_2 and Ag–ZrO_2 composite coatings were prepared by PLD. The structural and surface topography of the coatings were studied by XRD and AFM, respectively. Coating's thickness and morphology were analyzed by SEM. Elemental composition and mapping were analyzed by EDS. The efficiency of antibacterial properties of ZrO_2 and Ag–ZrO_2 composite coatings were evaluated and compared against *E.coli* and *S.aureus* bacteria.

Methods

Substrate pretreatment

Medical grade stainless steel 316L (316L SS) and silicon substrate (for characterization) were selected as a substrate and pretreatment was performed. Briefly, substrates were cut into $1 \times 1\ cm^2$ using automated cutting machine (Struers, Tegramin-25, Denmark). Mirror polishing was done using automated polishing machine (Struers A/S, DK-2750 Ballerup, Denmark) and silicon carbide emery papers (240–1000 mesh sizes) were used to reduce the surface roughness of the substrates. Finally, mirror polished substrates were treated with trichloroethylene in order to remove the rust and ultrasonicated for 15 min before coatings.

Deposition of silver-ZrO_2 composite coatings and their characterizations

The commercial ZrO_2 powders with 99.99 % purity were pressed with 40 MPa in the 8 mm mold to prepare disc. This disc was subjected to heat treatment at 900 °C for 5 h in air atmosphere with heating rate of 10 °C/min. The resultant 8 mm diameter and 3 mm thickness ZrO_2 disc and commercial silver with 25 mm diameter and 2 mm thickness disc were used as targets in this experiment. The vacuum chamber was evacuated by air cooled turbo-molecular pump and kept at 1×10^{-6} m bar as a base pressure as well as deposition pressure. A Q-switched Nd-YAG laser operating at wavelength 355 nm with fluence of 2 J/cm^2 and repetition rate of 10 Hz is allowed into the chamber through a quartz window. The laser beam with 2 mm diameter is focused on the targets at the angle of 45°. For Ag–ZrO_2 composites coatings, same 8 mm diameter ZrO_2 target is fixed on 25 mm Ag target (Fig. 1). Target and substrate distances were kept at 45 mm. Prior to deposition, both targets were ablated with 3,000 pulses to remove the surface contamination to get high-purity coatings with shutter between targets and substrates and 45,000 pulses have been applied on target for each coating. The substrates were kept at a constant temperature of 200 °C with ramping rate of 10 °C/min for both the deposition. Both depositions are performed at similar conditions.

The phase structure of ZrO_2 and Ag–ZrO_2 composite coatings were analyzed by glancing angle X-ray diffractometer (Rigaku, smart lab 9 KW, japan) using a CuKα = 1.5406Å radiation source. The surface of the
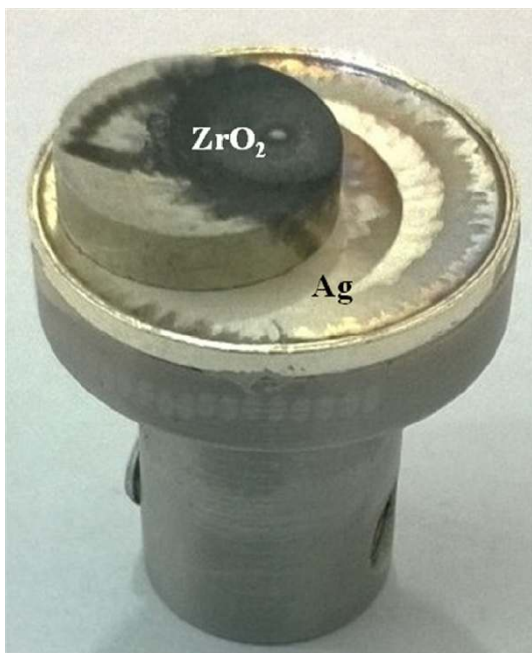
Fig. 1 Target holder consists of Ag and ZrO$_2$

coating was characterized by molecular imaging atomic force microscopy (AFM) using SLOVER PRO, multi mode scanning probe microscope manufactured by M/s NTMDT, the Irelands.

Bacterial adhesion study

Bacterial strains

E.coli (MTCC 443) and *S.aureus* (MTCC 3160) bacterial strains were used for this study. Cultures were maintained on nutrient broth at 37 °C.

Preparation and inoculation of organisms

The bacterial suspensions were prepared by taking a single colony from the stock bacterial culture with a loop and inoculating 20 ml of sterile nutrient broth in a 100-ml Erlenmeyer flask. The flask was then incubated in a shaking incubator at 37 °C at 110 rpm for 12 ± 2 h. After incubation, 0.4 ml of the overnight inoculum was transferred to a 100-ml Erlenmeyer flask containing 20 ml nutrient broth and incubated in a shaking incubator for 3 h at 37 °C and 110 rpm. The number of bacteria in the 3 h culture was estimated by measuring the optical density of the culture at 660 nm (Corning colorimeter 253). An optical density of between 0.1 and 0.3 was roughly equal to a concentration 2.5×10^8 CFU/ml.

Sterilizations of test samples

ZrO$_2$ and Ag–ZrO$_2$ composite onto 316L SS were sterilized under UV lamp with 5 cm distance for 10 min to obtain surface sterilization. Post exposure, specimens were transferred to sterilized disposable petriplates to avoid cross contamination. All the specimens were retained in the petriplates during each experiment.

Antibacterial analysis

The cultured bacterial strains were inoculated in 10 ml phosfate-buffered saline (PBS; g/l: KCl 0.2, KH$_2$PO$_4$ 0.2, NaCl 8.0, Na$_2$HPO$_{4.12}$H$_2$O) solution to reach approximate target concentration of 1×10^5 colony forming units/milliliter (CFU/ml). The saline solution containing bacteria was used for the 'drop-method' antibacterial experiments (Sun et al. 2008). The samples were placed in the sterilized petridishes. Then 100 µl of saline solution containing bacteria was added dropwise onto the surface of each deposited film. The samples were laid at ambient temperature for 12 h to evaluate absolute initial antimicrobial properties of test specimens. Incubated samples were washed with 5 ml of PBS in the sterilized petridish. Then 10 µl each of bacteria suspension was dispersed on the culture medium and incubated for 24 h at 37 °C. After that, Total viable count (TVC) was enumerated to evaluate viable bacterial cells arising from solid medium. The number of bacteria-forming units (CFU) was counted, and the reduction of bacteria, R, was calculated from

$$R = \frac{(B - A)}{B} 100 \, (\%), \tag{1}$$

where A is the CFU recovered from the uncoated 316L SS (data is not shown) and B is the CFU recovered from the coated samples over the desired contact period (24 h).

For live/dead cell analysis, same quantity of bacterial suspension was poured onto test specimens for 30 min. The incubated samples were gently washed in PBS to remove the unbound bacterial cells. Finally, acridine orange (AO) was added onto specimens and observed using Nikon Eclipse E600 Epifluorescence microscope (excitation filter BP 490; barrier filter O515).

Results and discussion

Figure 2 shows X-ray diffraction patterns of ZrO$_2$ and Ag–ZrO$_2$ composite coatings deposited at 200 °C onto 316L SS substrate with parallel-beam (PB) diffraction geometry. ZrO$_2$ coating shows the diffraction at (002), (102), (112), (221), (202) and (302) with corresponding 28.15, 33.92,
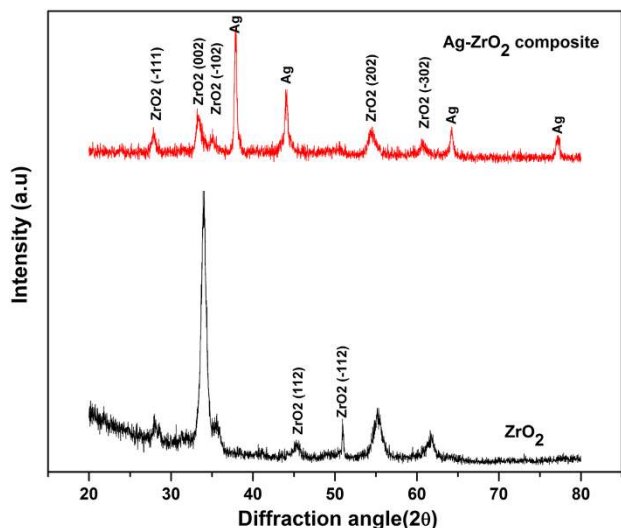
Fig. 2 XRD pattern of ZrO_2 and Ag–ZrO_2 composite coatings

35.56, 45.32, 50.87, 55.19 and 61.66° 2θ positions. Ag–ZrO_2 composite coatings can also be identified with (111), (002), (−102), (112), (−221), (202) and (302) planes with corresponding 2θ position of 27.95, 33.30, 35.15, 37.93, 44.09, 54.47, 60.74, 64.24 and 77.19°. For the estimation of average crystalline size, the following Scherrer equation is employed (Suryanarayan and Norton 1998).

$$t = 0.9\lambda/\beta \cos\theta \qquad (2)$$

where λ = wavelength of X-ray source, β = full width half maximum (FWHM) corresponding to XRD peaks.

The crystalline size of ZrO_2 is calculated from its peak broadening and crystalline size found to be 16.19 nm. In case of Ag–ZrO2 composite coatings, crystalline size of ZrO_2 found to be 13.56 nm. The crystalline of Ag was calculated as 27.14 nm and no secondary phase of Ag was observed. It clearly indicates that crystallinity of Ag fully improved and crystalline size was larger than that of ZrO_2. At this low substrate temperature (200 °C), some grains of the ZrO_2 material grows amorphous nature, whereas Ag grain growth fairly formed crystalline nature and this formation inhibited further grain growth of ZrO_2 in Ag–ZrO_2 composite coatings.

Typical nano topography using two-dimensional (2D) and three-dimensional (3D) images of AFM with surface profiles of ZrO_2 and silver-ZrO_2 composite coatings are shown in Figs. 3, 4. A comparative AFM analysis indicated that the slightly heterogeneous surface with increased grains exhibited in ZrO_2 coating; for Ag–ZrO_2 composite coatings, homogenous surfaces with fine topographical alterations are observed. The degree of roughness and grains in ZrO_2 coating (R_a = 1.4541 nm) is slightly increased than silver-ZrO_2 (R_a = 1.04816 nm) coatings. ZrO_2 coatings showed the maximum and minimum grain

sizes in the range of 4–10 nm along with few agglomerations. For Ag–ZrO_2 composite, it has shown as 3–8 nm. From 2D and 3D profile of AFM surface profile analysis concludes that the addition of silver content in ZrO_2 results in a minute decrease of both the grain size and surface roughness due the nucleation matter (Subramanian and Jayachandran 2007).

Morphology as well as cross section of the ZrO_2 and Ag–ZrO_2 composite coatings is shown in Fig. 5. Both ZrO_2 (Fig. 5a) and Ag–ZrO_2 (Fig. 5b) composite coatings showed dense, smooth and defect-free surface along with smaller grain size. Few droplets or agglomeration of grains was also observed in both coatings. Formation of droplets is one of the intrinsic properties of laser ablation technique (Willmott and Huber 2000). The total thickness of the ZrO_2 and Ag –ZrO_2 composite coatings is evaluated from the cross-sectional view of the samples and found to be 120 and 154 nm, respectively. The slight variation of thickness attributed to the difference in ablation rate of Ag and ZrO_2. Generally, pure metals have more ablation rates than ceramic materials in PLD technique. In this case the ablation rate of metallic Ag is comparatively more than that of ZrO_2 ceramic material.

Figure 6 shows the compositional analysis of ZrO_2 coatings contains both zirconium (Zr), oxygen (O) and silicon (Si). Figure 7 shows the compositional analysis and elemental mapping of Ag–ZrO_2 composite coatings, in which, the wt % of Ag was 1.17. Si peak was also observed due to the surface effect. From the compositional analysis, the presence of Zr, O and Ag, Zr, O were confirmed in ZrO_2 and Ag–ZrO_2 composite coatings.

Antimicrobial activity of ZrO_2 and Ag–ZrO_2 composite coatings coated 316L SS was evaluated by determining TVC. ZrO_2 coating shows antibacterial activity of about 99 % (data are not shown) against *E.coli* and exhibits very less antibacterial efficiency about 46 % against *S.aureus*. On the other hand, drastic growth arrest is observed on Ag–ZrO_2 composite coatings with the antimicrobial efficiency of 99.5 and 99 % for *E.coli* and *S.aureus*, respectively. During incubation, when aqueous bacterial solutions are exposed onto coating surfaces, many of the bacteria have a possibility to attach directly to the surface. Since silver is present on the surface of the samples, metallic silver ions leached from coating surface and affect both adhered and non adhered bacterial cell wall (Sondi and Sondi 2004). The mechanism of both bacterial strains against Ag–ZrO_2 composite coatings varies as (a) Ag ions may bind with bacterial cell surface proteins such as porins, OmpF and OmpC and produce imbalanced membrane diffusion in gram-negative bacteria; (b) metallic Ag ions bind with surface anionic proteins and lost their membrane rigidity and increase the cell wall porosity. Hence, the above mechanisms elevate oxidative stress;
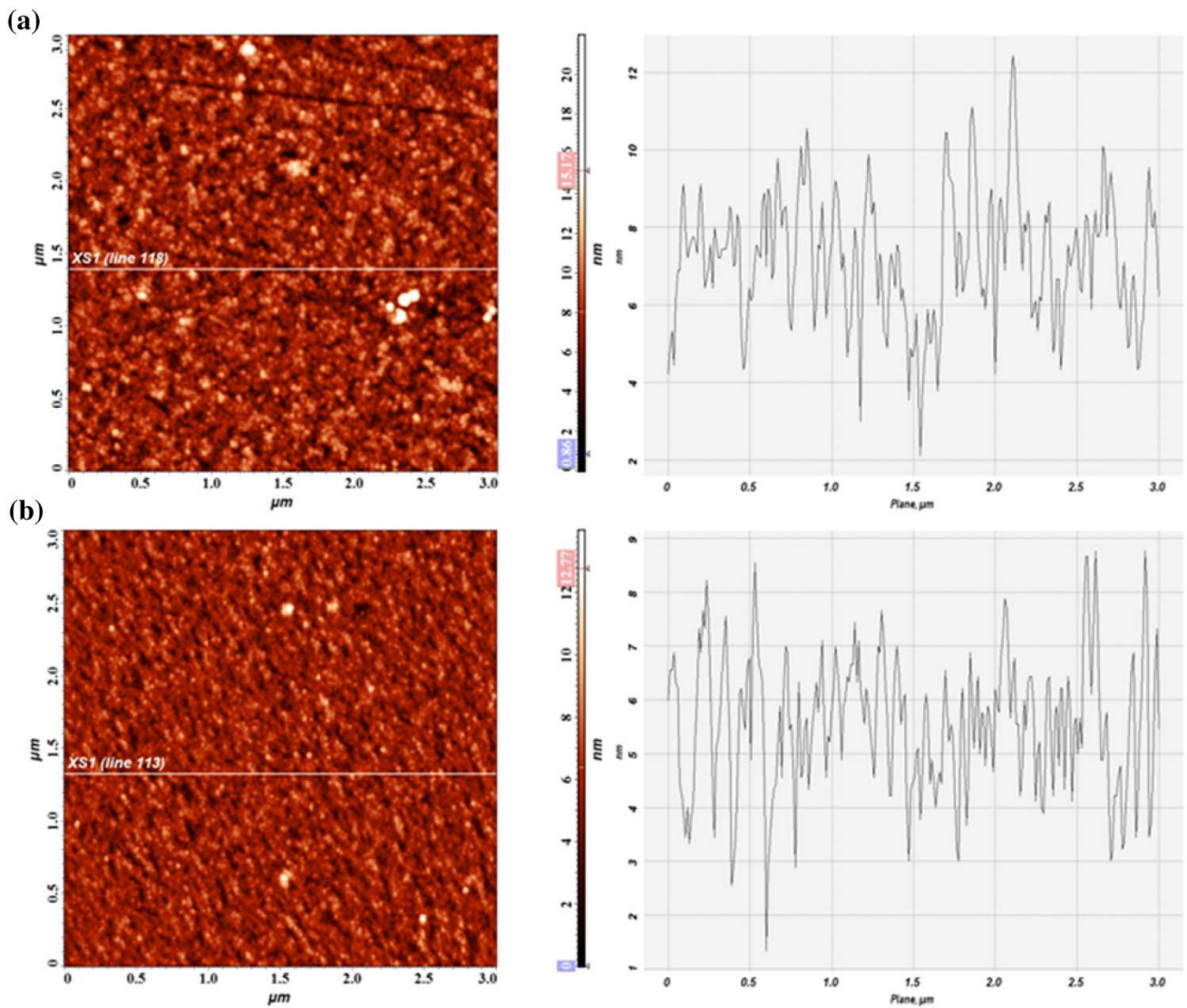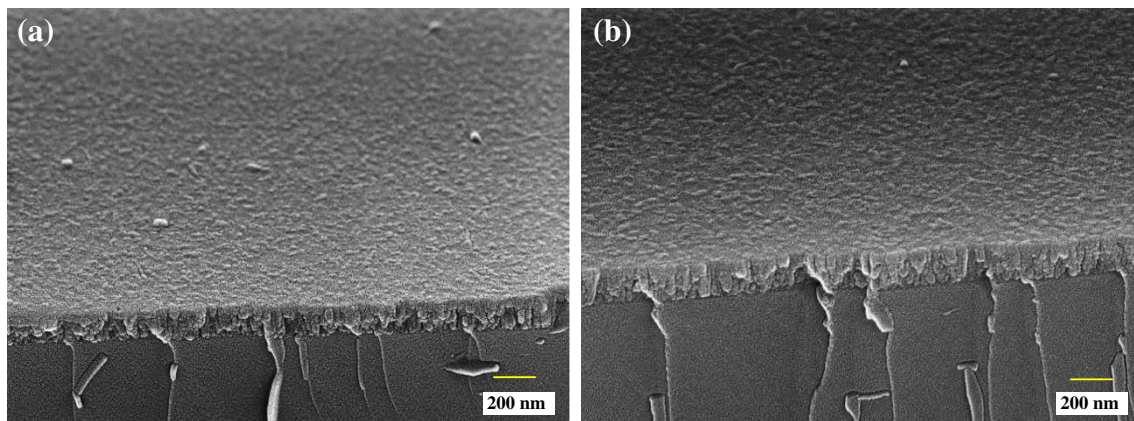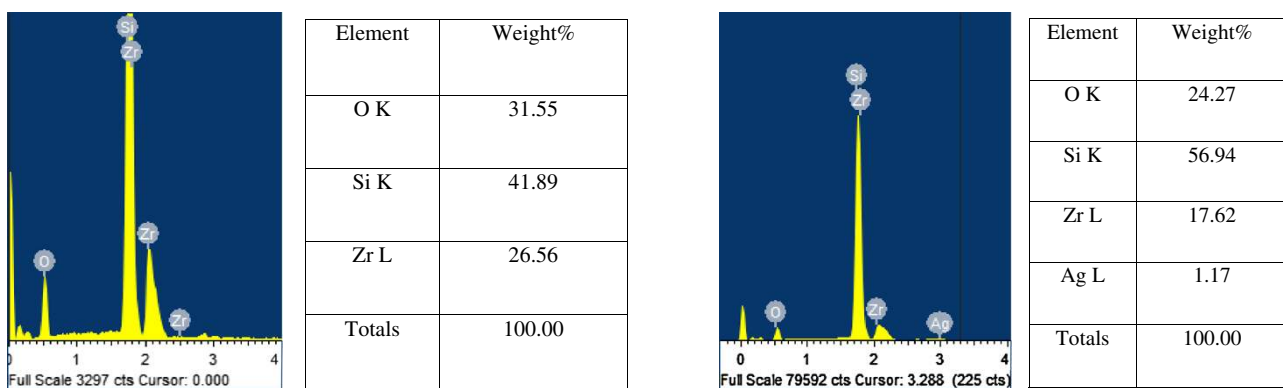
Fig. 3 Two-dimensional (2D) AFM images and surface profiles of ZrO₂ (**a**) and Ag–ZrO₂ composite coatings (**b**) coated 316L SS from approximately 3 × 3 μm scanned areas
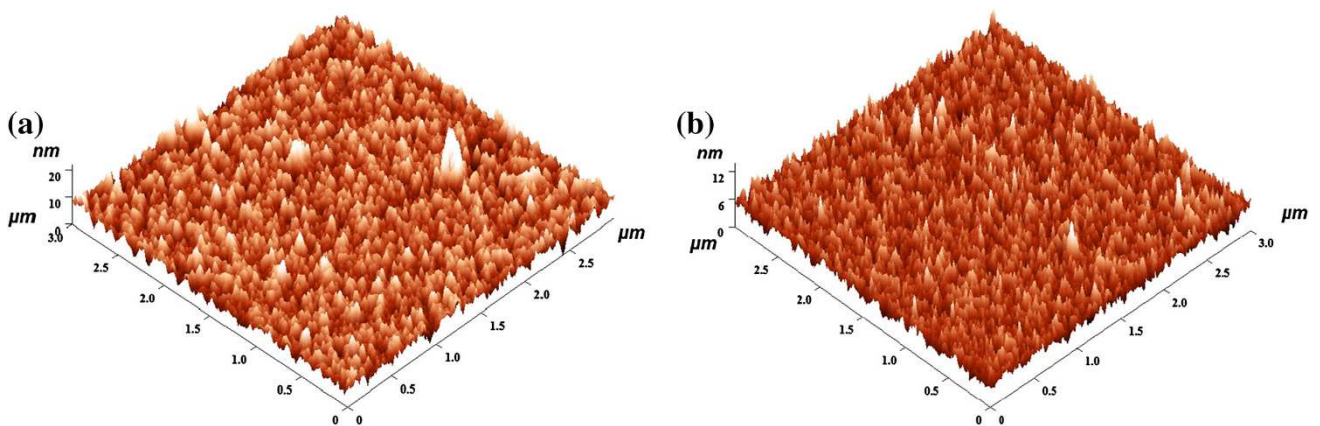
Fig. 4 Three-dimensional (3D) projections of typical AFM images and surface profiles of ZrO₂ (**a**) and Ag–ZrO₂ composite coatings (**b**) coated 316L SS from approximately 3 × 3 μm scanned areas
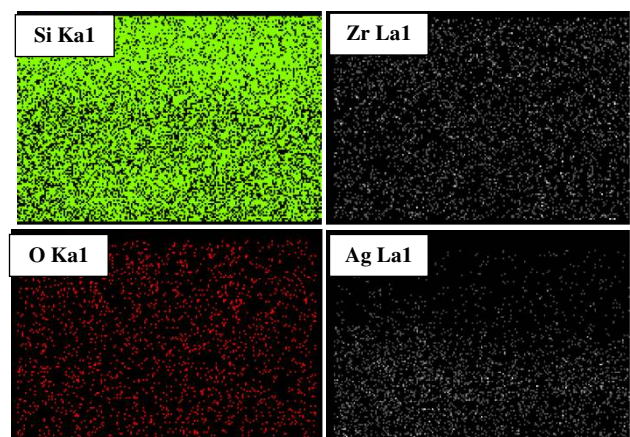
Fig. 5 Cross-sectional images of ZrO_2 and Ag–ZrO_2 composite coatings

Element	Weight%
O K	31.55
Si K	41.89
Zr L	26.56
Totals	100.00

Fig. 6 Compositional analysis of ZrO_2 coating

Element	Weight%
O K	24.27
Si K	56.94
Zr L	17.62
Ag L	1.17
Totals	100.00

Fig. 7 Elemental and compositional analysis of Ag–ZrO_2 composite coating

thereby free radicals production occurs which arises reactive oxygen species, resulting structural changes and cell damage occur. In addition to that, the metallic silver ions are effectively involved in binding with sulfur or phosphorus-containing soft bases, such as R-S-R, R-SH, RS^- or PR_3 which is present in cell membrane and phosphate group of DNA which is located inside the cell (Bragg and Rainnie 1974; McDonnell and Russell 1999; Darouiche 1999). As a result, the bacterial growth is effectively inhibited within a short time of exposure. From the TVC results, it could be speculated that ZrO_2 coating worked out exhibited better antibacterial activity only against *E.coli* and no activity for *S.aureus*. It is due to the heterogeneity structure and chemical composition of the outer membrane of gram +ve and gram −ve bacteria (Thomas et al. 2010). The calculated TVC of gram (−)ve and gram (+)ve test organisms are to be 1.78×10^2, 1.02×10^4 for ZrO_2 coating and 92, 164 for Ag–ZrO_2 composite coatings, respectively.
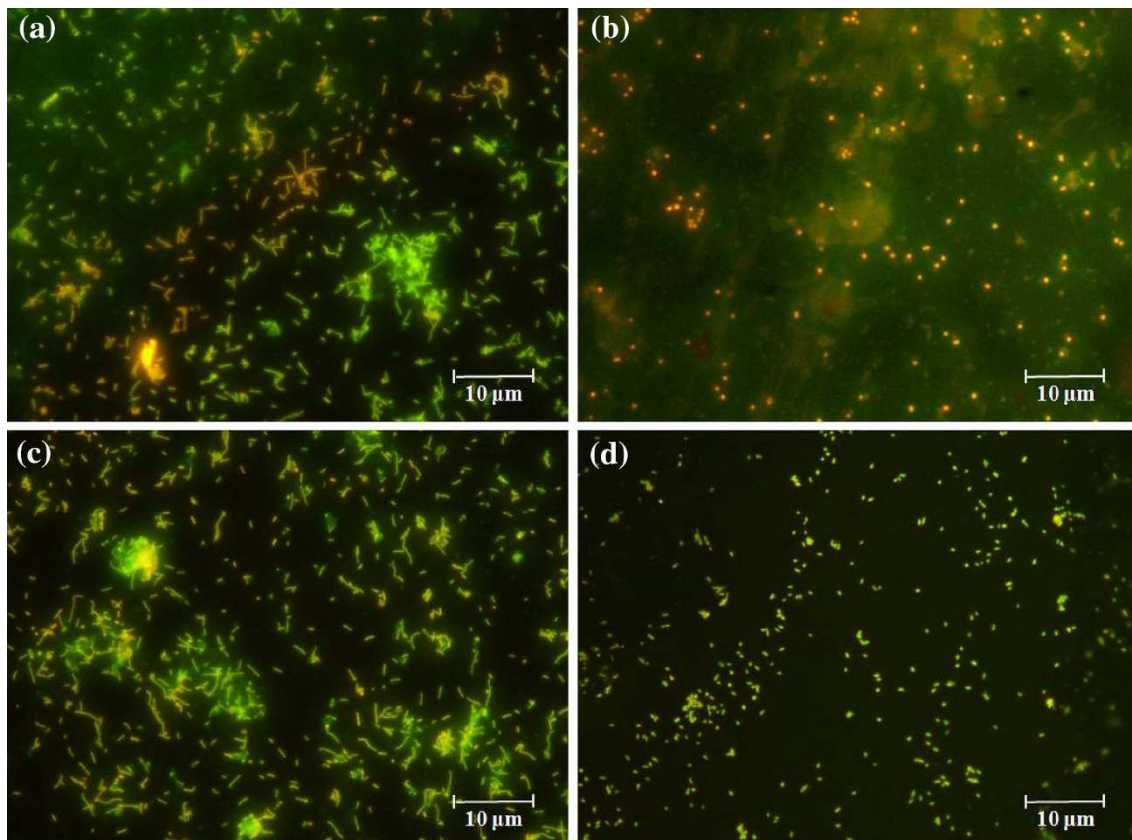
Figure 8 depicts epifluorescence microscopy images of ZrO_2 and Ag–ZrO_2 composite coated 316L SS. In principle, live cells exhibited orange fluorescence and dead cells

exhibited green color due to the interaction of AO with cellular RNA (Vinita Vishwakarma et al. 2009). Epifluorescence results exhibited similar results with TVC analysis. Bacterial inoculated ZrO_2 coating shows green fluorescence for *E.coli* bacteria; orange color fluorescence for *S.aureus*. Result concludes that ZrO_2 coating shows bacterial activity against *E.coli* and fails to express the

Fig. 8 Epifluorescence microscopy images of ZrO$_2$ (Fig. 5a *E.Coli* and **b** *S.aureus*) and Ag–ZrO$_2$ composite coatings (Fig. 5c *E.Coli* and **d** *S.aureus*)

bactericidal nature against *S.aureus*. In case of Ag–ZrO$_2$ composite coatings, both *E.coli* and *S.aureus* show green fluorescence indicates dead cells. The exposed bacteria are interacting with Ag ions which undergo severe changes in and around the bacterial cell wall thereby elevating deterioration of bacterial cell wall. Besides, strong interaction of silver ions with intracellular components affects further cellular RNA synthesis which leads bacterial death.

Conclusions

ZrO$_2$ and Ag–ZrO$_2$ composite coatings were successfully prepared using PLD technique. XRD examination reveals that monoclinic phase for ZrO$_2$ and mixed phase for Ag–ZrO$_2$ composite coatings were obtained. AFM morphology of the coatings clearly indicated that the grains are evenly distributed. Elemental analysis by EDS confirmed the presence of Ag in Ag–ZrO$_2$ composite coatings about 1.17 wt % of Ag. The antimicrobial efficiency was performed using TVC and epifluorescence microscopy analysis in which Ag–ZrO$_2$ composite coatings shows superior antibacterial when compare to ZrO$_2$ coating. Hence, the 1.17 wt % Ag content exhibits superior antibacterial activity

and it may be the good candidate for biomedical applications.

References

Arisara T, Virote B, Nirun W (2012) Apatite deposition on ZrO$_2$ thin films by DC unbalanced magnetron sputtering. Advan Mater Physic Chem 2:45–48

Atiyeh BS, Costagliola M, Hayek SN, Dibo SA (2007) Effect of silver on burn wound infection control and healing: review of the literature. Burns 33:139–148

Bragg PD, Rainnie DJ (1974) The effect of silver ions on the respiratory chains of *Escherichia coli*. Can J Microbiol 20:83–889

Chen W, Oh S, Ong AP, Oh N, Liu Y, Courtney HS, Appleford M, Ong JL (2007) Antibacterial and osteogenic properties of silver-containing hydroxyapatite coatings produced using a sol gel process. J Biomed Mater Res A 82A:899–906

Chevalier J (2006) What future for zirconia as a biomaterial? Biomat 27:535–543

Darouiche RO (1999) Anti-infective efficacy of silver-coated medical prostheses. Clin Infect Dis 29:1371–1377

Ewald A, Gluckermann SK, Thull R, Gbureck U (2006) Antimicrobial titanium/silver PVD coatings on titanium. Biomed Eng Online 5:1–10

Gu FX, Karnik R, Wang AZ, Alexis F, Nissenbaum EL, Hong S, Langer RS, Farokhzad OC (2007) Targeted nanoparticles for cancer therapy. Nanotoday 2:14–21

Holleck H (1991) Designing advanced coatings for wear protection. Surf Eng 7(2):137–144

Jangra SL, Stalin K, Dilbaghi N, Kumar S, Tawale J, Singh SP, Pasricha R (2012) Antimicrobial activity of zirconia (ZrO_2) nanoparticles and zirconium complexes. J Nanosci Nanotech 12(7105–7):112

Jelinek M, Kocourek T, Remsa J, Weiserova M, Jurek K, Miksovsky J, Strnad J, Galandakova A, Ulrichova J (2013) Antibacterial, cytotoxicity and physical properties of laser—Silver doped hydroxyapatite layers. Mater Sci Eng C 33:1242–1246

Kokubo T (2008) Bioceramics and their clinical applications. Woodhead, England

Lansdown ABG (2006) Silver in health care: antimicrobial effects and safety in use. Curr Probl Dermatol 33:17–34

Lansdown AB (2007) Critical observations on the neurotoxicity of silver. Crit Rev Toxicol 37:237–250 Lansdown 2007

McDonnell G, Russell AD (1999) Antiseptics and disinfectants: activity, action, and resistance. Clin Microbiol Rev 12:147–179

Nathan AT, Rachael AO, Hongyan Ma, James DB, John DW, Ketul CP (2012) Antibacterial effects of silver-doped hydroxyapatite thin films sputter deposited on titanium. Mater Sci Eng C 32:2135–2144

Sondi Sondi BS (2004) Silver nanoparticles as antimicrobial agent: a case study on *E. coli* as a model for Gram-negative bacteria. J Colloid Interface Sci 275:177–182

Subramanian B, Jayachandran M (2007) Characterization of reactive magnetron sputtered nanocrystalline titanium nitride (TiN) thin films with brush plated Ni interlayer. J Appl Electrochem 37:1069–1075

Sun SQ, Sun B, Zhang W, Wang D (2008) Preparation and antibacterial activity of Ag–Tio2 composite film by liquid phase deposition (LPD) method. Bull Mater Sci 31:61–66

Suryanarayan RC, Norton MG (1998) X-ray diffraction: a practical approach. Plenum Press, New York

Thomas JS, Daniel K, Suzanne W (2010) The bacterial cell envelope. Cold Spring Harb Perspect Biol 2:1–16

Uchida M, Kim HM, Kokubo T, Tanaka K, Nakamura T (2002) Structural dependence of apatite formation on zirconia gels in a simulated body fluid. J Ceram Soc Japan 110:710–715

Udo G (2009) Pathogenic organisms in hip joint infections. Int J Med Sci 6:234–240

Vishwakarma Vinita, Josephine J, George RP, Krishnan R, Dash S, Kamruddin M, Kalavathi S, Manoharan N, Tyagi AK, Dayal RK (2009) Antibacterial copper-nickel bilayers and multilayer coatings by pulsed laser deposition on titanium. Biofoul 25:705–710

Willmott PR, Huber JR (2000) Pulsed laser vaporization and deposition. Rev Modern Physic 72:315–328

Zheng X, Chen Y, Xie Y, Ji H, Huang L, Ding C (2009) Antibacterial property and biocompatibility of plasma sprayed hydroxyapatite/silver composite coatings. J Therm Spray Technol 18:463